ELSEVIER

Catalysis Today 54 (1999) 465–472

CATALYSIS TODAY

www.elsevier.com/locate/cattod

EPR spectroscopic characterization of $DeNO_x$ and SO_2 oxidation catalysts and model systems

K.M. Eriksen [a,*], C.K. Jensen [a], S.B. Rasmussen [a], C. Oehlers[a,1], B.S. Bal'zhinimaev [b], R. Fehrmann [a]

[a] *Department of Chemistry, Technical University of Denmark, DK-2800 Lyngby, Denmark*
[b] *Boreskov Institute of Catalysis, 630090 Novosibirsk, Russia*

Abstract

The industrial SO_2 oxidation catalyst VK69 deactivates at around 440°C in a 10% SO_2, 11% O_2, 79% N_2 gas mixture. In situ EPR measurements show that the deactivation is caused by the precipitation of V(IV) compounds. $DeNO_x$ catalysts based on V_2O_5/TiO_2, the TiO_2 support, analytical grade anatase and transition metal-exchanged Al-PILCs (pillared clay) have been characterized by EPR spectroscopy and the catalytic activity of the catalysts monitored up to 500°C. Depending on the exchanged metal ion, a relatively large temperature range for the catalytic activity towards the SCR reaction was observed.

Keywords: $DeNO_x$ and SO_2 oxidation catalysts; Anatase; EPR characterization; Deactivation

1. Introduction

Catalysts for SO_2 oxidation and NO_x reduction are important for the catalytic removal of acidic pollutants from industrial off-gases. The industrial SO_2 oxidation catalyst is based on V_2O_5 and usually promoted by a mixture of alkali salts. During operation at 400–600°C, the conversion of SO_2 and O_2 to SO_3 leads to the formation of a pyrosulfate melt in the pores of the support. V_2O_5 dissolves in the melt and forms vanadium oxo–sulfato complexes (e.g. $V_2O_5 + S_2O_7^{2-} \rightleftharpoons 2VO_2SO_4^-$), where vanadium is found in the oxidation states V, IV and III [1–5]. The structure of these complexes in the catalyst melt is currently under investigation [6–9]. By lowering the temperature below ~430°C the catalyst deactivates due to the precipitation of V(IV) and/or V(III) compounds [10–12].

Industrial $DeNO_x$ catalysts are usually based on V_2O_5 with additives of WO_3 or MoO_3 supported on solid TiO_2 (anatase). The mechanism of the SCR of NO_x, by injection of NH_3 in the flue gas, has been studied in detail recently [13]. However, the possible reduction of V(V) to V(IV) and V(III) as well as Ti(IV) to Ti(III) of the TiO_2 support during the SCR reaction has not, as far as we know, been studied by EPR in situ at temperatures up to 500°C. Previous EPR investigations on V_2O_5/TiO_2 catalysts (e.g. [14–17]) and anatase in air, vacuum or reducing atmosphere (e.g. [14,18,19]) have only been performed at ambient or lower temperatures after cooling of samples treated at higher temperatures. Also zeolites and, recently PILC (pillared interlayered clays) [20], have attracted much

* Corresponding author.
[1] Present address: BP Chemicals Limited, Research Laboratory, Poplar House, Chertsey Road, Sunbury-on-Thames, Middlesex TW16 7LL.

0920-5861/99/$ – see front matter
PII: S0920-5861(99)00209-6

attention due to their possible use in various off-gases and temperature ranges where the V_2O_5/TiO_2 catalyst has low activity.

The present work is concerned with in situ and room-temperature EPR investigations of the redox and structural chemistry of these important environmental catalysts.

2. Experimental

2.1. SO_2 oxidation catalyst

The industrial catalyst VK 69 (Haldor Topsøe A/S, Denmark) consists of V_2O_5 on kieselguhr, promoted by an alkali salt mixture containing Na, K and Cs.

2.2. V_2O_5/TiO_2 $DeNO_x$ catalysts

The investigated $DeNO_x$ catalysts were, respectively, composed of 3.6 w/w% V_2O_5 + 7.8 w/w% WO_3 (Russian industrial catalyst) and 6.0 w/w% V_2O_5 (Haldor Topsøe A/S, laboratory catalyst), both on TiO_2. The investigated anatase (TiO_2) was from Aldrich (>99.9%).

2.3. PILC catalysts

The 'pillared clay' catalysts were prepared from bentonite clay (Sigma). For the preparation of Al-PILC, a commercial Al-chloride solution, Lochron-L, Hoechst ($[Al^{3+}] = 4.6$ M, OH/Al = 2.5) was used as pillaring agent. Thereafter, 4.6 ml of this solution were mixed with 275 ml of water and 5 ml of 0.6 M HCl. The pH of the solution was 3.8. Next, 10 g of clay were added to the pillaring solution and mixed for 4 h. After separation and washing until chloride-free, the exchanged clay was air-dried. Calcination was performed in air at a heating rate of 2°C/min up to 500°C. This temperature was maintained for 3 h.

LaAl-PILC was prepared according to the method of Sterte [21]. The pillaring solution was prepared by hydrothermal treatment of a solution containing aluminum chlorohydrate (Lochron-L, Hoechst) and lanthanum chloride. Then, 10.5 g of $LaCl_3$ were added in a solution containing 43.5 ml Lochron-L and 36.5 ml water. The experiments were all performed using an Al concentration of 2.5 M and an La/Al molar ratio of 1/5. The OH/Al molar ratio was 2.5. The hydrothermal treatment was carried out in a stainless steel autoclave at 120°C or by refluxing the solution for 96 h. Thereafter, 10 g of clay were dispersed in 500 ml water and stirred for 5 h. The pillaring solution was added and stirred for another hour. The amount of aluminum per gram of clay was 20 mmol. The product was washed, air-dried and calcined as described for the Al-PILC preparation.

Transition metal-containing PILCs were prepared by exchanging transition-metal cations into the PILC by a two-step method [22]. First, calcined PILCs were treated with an aqueous solution containing sodium cations at various pH to restore the cation exchange capacity (CEC). Then the sodium PILC was exchanged with an aqueous solution of the desired transition-metal cations, like Cu(II), Ni(II) and Cr(III), at a pH of about 3 to 5 to restore the sodium cations.

2.4. EPR measurements

A Bruker EMX equipped with a Bruker ER 4114HT X-band cavity or a JEOL JES-ME 1X EPR spectrometer equipped with a Bruker ER 4114HT X-band cavity was used for high-temperature EPR measurements. The experimental setup for in situ EPR spectroscopy and simultaneous measurement of the catalyst activity has been described earlier in detail [10–12]. The crushed catalyst samples (up to around 50 mg) were contained in the inner tube of a reactor cell consisting of two concentric quartz tubes (i.d. 1.8 and 3 mm, respectively). The reactor cell was placed in the high-temperature cavity, where heating up to 1200 K is possible. The inlet gas was preheated by passing through the outer tube before entering the inner tube with the catalyst sample fixed in position by small quartz wool plugs. The temperature was measured by a 1/16 in. Chromel–Constantan thermocouple placed on top of the catalyst sample. The NO and SO_2 concentration in the gas could be analyzed by UV spectrophotometry before, and after, passing the sample.

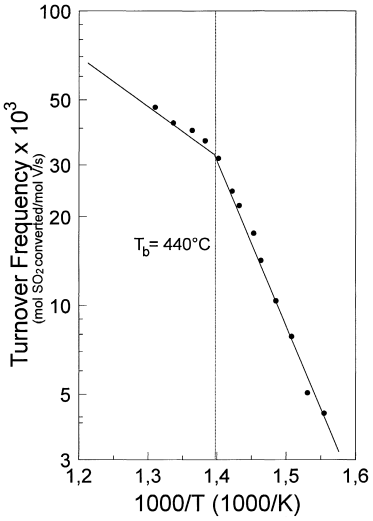

Fig. 1. Arrhenius-type plots for the industrial sulfuric acid catalyst VK69 in 10% SO_2, 11% O_2 and 79% N_2 (raw synthesis gas).

3. Results and discussion

3.1. SO_2 oxidation catalysts.

The industrial SO_2 oxidation catalyst, VK69, has been investigated in 10% SO_2, 11% O_2-, 79% N_2-simulated sulfuric acid synthesis gas at temperatures up to 500°C. The conversion of SO_2 was below ≈30%, and considered differential, obtained at a gas flow of around 20 ml/min. An Arrhenius-type plot of the activity vs. $1/T$ is shown in Fig. 1. The breakpoint temperature, T_b, is observed at 440°C, and is in good accordance with earlier [10] measurements on industrial catalysts. Below T_b, the activity decreases steeply most probably due to the precipitation of V(IV) or V(III) compounds from the catalyst melt [5,10]. The in situ EPR spectra of the VK69 catalyst are shown in Fig. 2 in the same temperature range as the activity measurements. At high temperatures, a broad line is observed with unresolved hyperfine structure as expected for a V(IV) polymeric complex, e.g. $(VO(SO_4)_2)_n^{2n-}$, in solution. Decreasing the temperature gives rise to an increase in the intensity of the broad line and the appearance of weak features of the eight-line spectrum characteristic of monomeric V(IV) complexes. This is in accordance with a shift of the redox equilibrium $V(V) + SO_2 \rightleftharpoons V(IV) + SO_3$ towards V(IV) by lowering the temperature [23]. The line

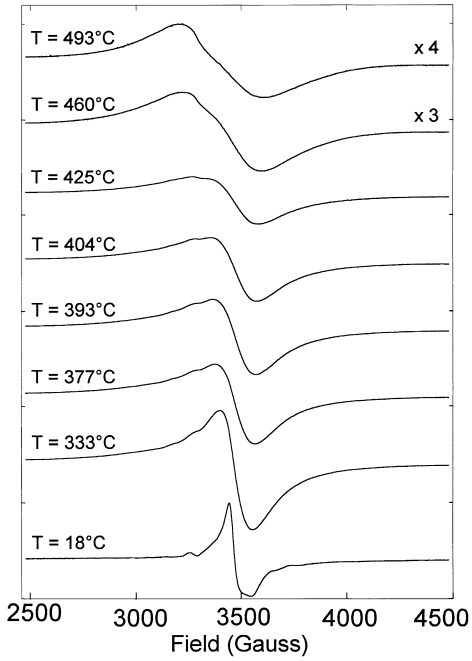

Fig. 2. EPR spectra of VK69 catalyst at various temperatures in 10% SO_2, 11% O_2 and 79% N_2 (raw synthesis gas). $\nu = 9.535$ GHz.

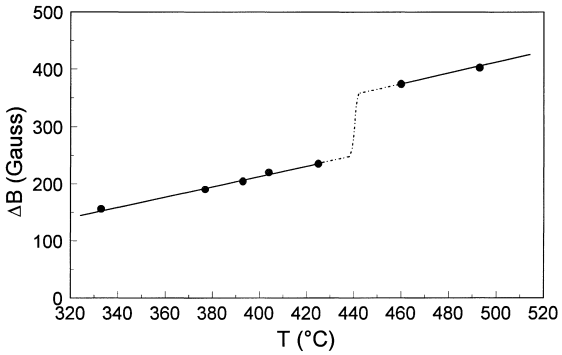

Fig. 3. Apparent linewidth ΔB vs. temperature. The dotted line represents the temperature, T_b, where the deactivation sets in. $\nu = 9.34$ GHz.

widths of the EPR spectra vs. the measuring temperature are shown in Fig. 3. A marked change of the line width is observed around 440°C, i.e. the breakpoint temperature found for the catalytic activity (Fig. 1). Below this temperature, the EPR spectra (Fig. 2) narrows and at room temperature it exhibits the features of V(IV) crystalline compounds [10]. A closer analysis reveals that the spectrum at 18°C most probably is composed of features from two V(IV) compounds

[10], i.e. $Cs_2(VO)_2(SO_4)_3$ and $K_4(VO)_3(SO_4)_5$. This is in agreement with preliminary EPR measurements on deactivated samples of VK69 from separate experiments performed in the EPR reactor cell, and in the cell used for activity measurements, which showed formation of $K_4(VO)_3(SO_4)_5$ and $Cs_2(VO)_2(SO_4)_3$, respectively. It can, therefore, be concluded that, as for example, small changes in gas flow and change of temperature in different steps may lead to the formation of different V(IV) compounds.

Based on the EPR spectra it, seems that in the present case $K_4(VO)_3(SO_4)_5$ precipitates first and then $Cs(VO)_2(SO_4)_3$ at lower temperatures, i.e. below 333°C. The precipitation of the V(IV) compounds results in a sharp decrease of the catalytic activity at T_b, the temperature where the precipitation sets in, depleting the melt also for the active V(V) species. As has been recently described [24], the catalytic activity is due to the presence of dissolved V(V) species, mainly as dimeric vanadium oxo–sulfato complexes.

3.2. $DeNO_x$ catalysts

The measured EPR spectra of the V_2O_5/TiO_2 catalyst (Topsøe) are shown in Figs. 4 and 5 and for the

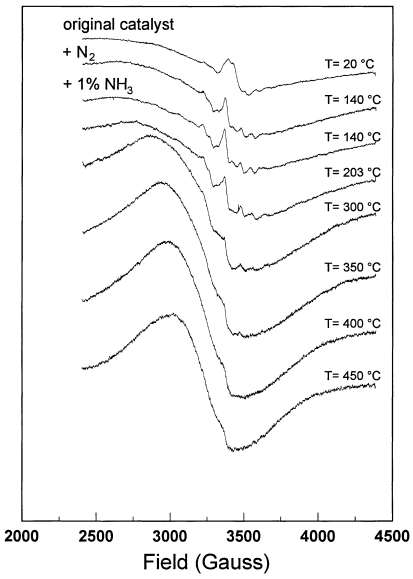

Fig. 4. EPR spectra of 6 w/w% V_2O_5/TiO_2 (Topsøe) in various gases (N_2, $N_2 + 1\%NH_3$) heated to the indicated temperatures. $\nu = 9.34$ GHz.

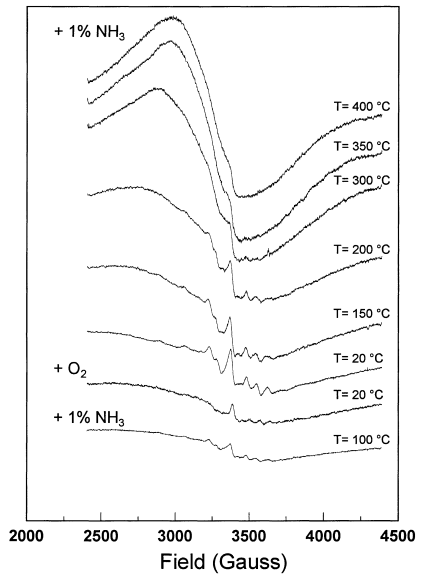

Fig. 5. EPR spectra of 6 w/w% V_2O_5/TiO_2 (Topsøe) in various gases ($N_2 + 1\%NH_3$, O_2) cooled to the indicated temperatures. $\nu = 9.34$ GHz.

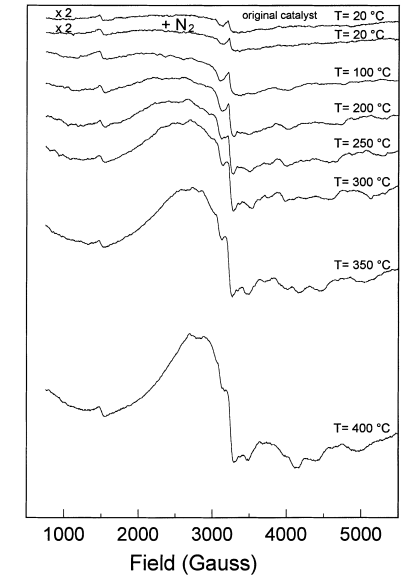

Fig. 6. EPR spectra of 3.6 w/w% $V_2O_5/WO_3/TiO_2$ (Russian industrial catalyst) in N_2(g) heated to the indicated temperatures. $\nu = 9.34$ GHz.

$V_2O_5 + WO_3/TiO_2$ (Russian industrial) in Figs. 6 and 7. The catalysts have been investigated in N_2, O_2 and 1% NH_3 in N_2, i.e. in neutral, oxidizing and reducing atmospheres in the temperature range 20–450°C. The

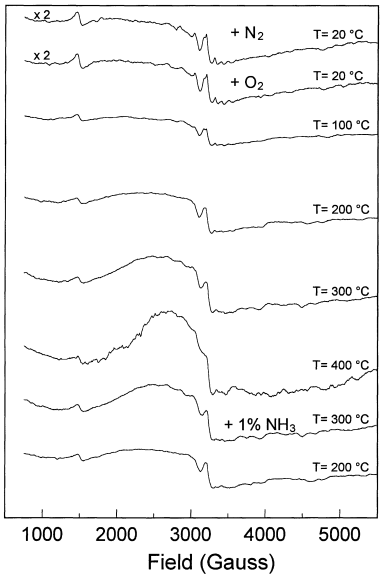

Fig. 7. EPR spectra of 3.6 w/w% $V_2O_5/WO_3/TiO_2$ (Russian industrial catalyst) in various gases (N_2 + 1%NH_3, O_2) heated and cooled to the indicated temperatures. ν = 9.34 GHz.

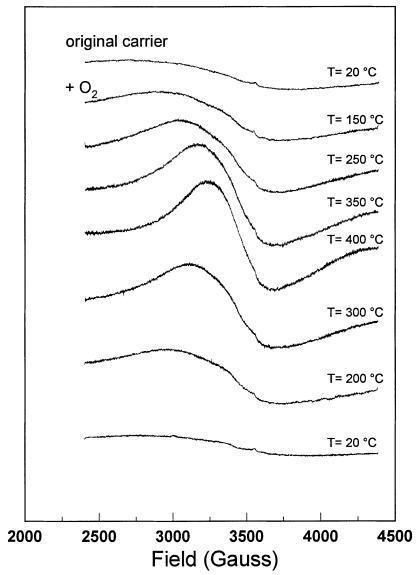

Fig. 8. EPR spectra of the industrial TiO_2 carrier (Topsøe) in O_2(g) at the indicated temperatures. ν = 9.34 GHz.

main features of the spectra of both catalysts include a broad temperature-sensitive line with line width in the range 500–1000 G and superimposed on this a number of small central lines that are temperature sensitive only to a limited degree. Fig. 10 shows a blowup

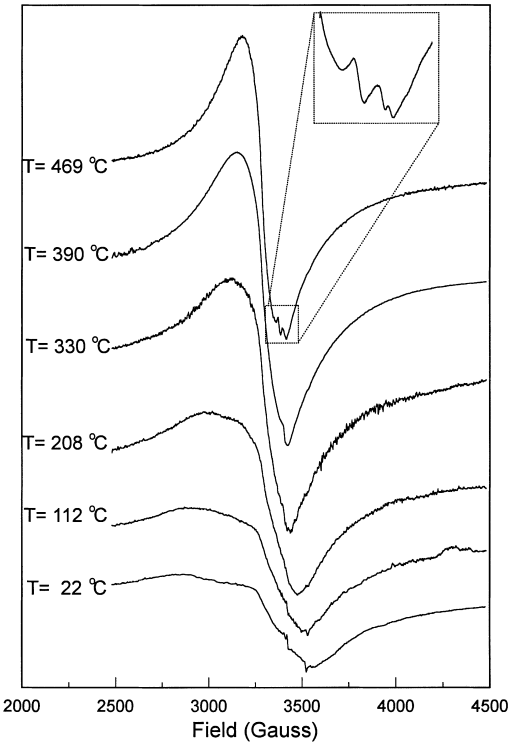

Fig. 9. EPR spectra of analytical grade TiO_2 (Anatase, Aldrich >99.9%) in air at the indicated temperatures. ν = 9.540 GHz.

of an EPR spectrum of the 6 w/w% V_2O_5/TiO_2 catalyst (Topsøe) at room temperature after treatment by a 0.05% NO, 0.07% NH_3, 2% O_2, N_2 (to balance)-gas mixture at 20–500°C. The hyperfine structure can be resolved into the indicated parallel and perpendicular components characteristic of isolated V(IV) $3d^1$ electronic species coupling with the ^{51}V nucleus with nuclear spin 7/2. The general features and the non-split perpendicular components point to the presence of isolated octahedral V(IV) complexes with high axial symmetry. Since the stability of these species does not seem much dependent on the gas mixture, whether reducing or oxidizing at all temperatures, they are probably formed in the TiO_2 matrix by diffusion of vanadium ions from the surface into the crystal lattice of the carrier. Spectra, very similar to that shown in Fig. 10, have earlier been obtained [25], but attributed to surface V(IV) species. However, the surface vanadium (IV) species are probably tetrahedrally coordinated so their EPR spectra are expected to be measurable only at very low temperatures, i.e. below 100 K.

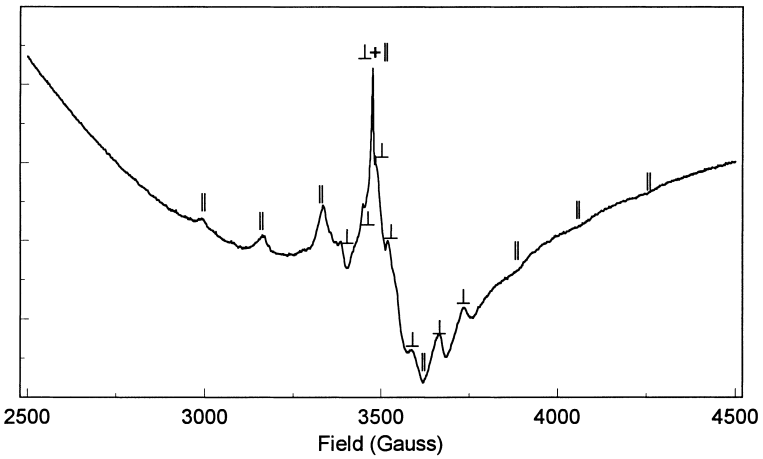

Fig. 10. EPR spectrum of 6 w/w% V_2O_5/TiO_2 (Topsøe) at room temperature after exposure to 0.05% NO, 0.07% NH_3, 2% O_2 in N_2 at 20–500°C. Catalyst mass 0.010 g, total flow rate 100 ml/min, $\nu = 9.759$ GHz.

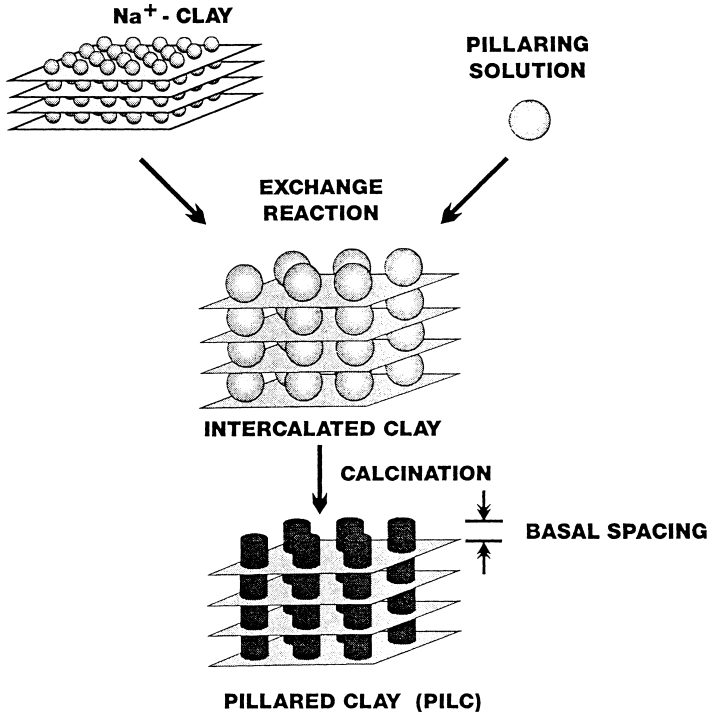

Fig. 11. Schematic structure of PILC.

This applies also for possible V(III) species formed. Such low-temperature investigations are in progress, as is a thorough, combined in situ EPR and activity study in simulated power plant flue gas and other industrial off-gases. The broad temperature-sensitive line of the EPR spectra of the catalysts has earlier [15] been attributed to polymeric V(IV) species, where coupling along the polymer chain smears out the hyperfine structure. However, the spectra displayed in Fig. 8 clearly show that the broad line is associated with the TiO_2 carrier alone. Even in O_2, a paramagnetic center is formed reversibly with respect to the temperature,

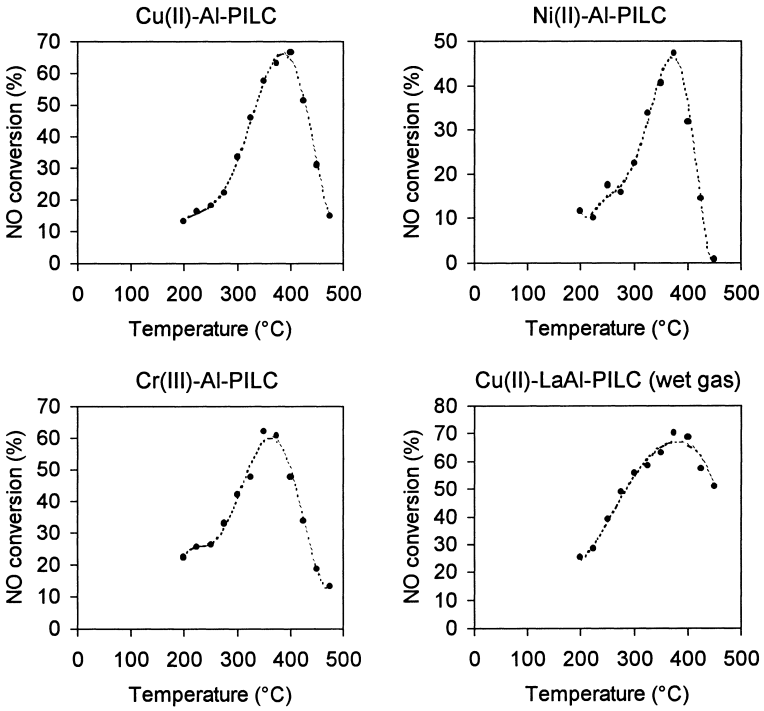

Fig. 12. SCR of NO by NH_3 on transition-metal ion-exchanged PILC in 0.05% NO, 0.05% NH_3, 2% O_2 and N_2 to balance. Catalyst mass 0.1 g, total flow rate 100 ml/min.

in the range 20–400°C. Since titanium oxides are well known to form non-stoichiometric compounds, this is probably also the case for the present industrial TiO_2 carrier.

Thus, oxidation states of Ti lower than +IV (i.e. +II or +III) might be present leading to a temperature-sensitive location of unpaired electrons in the structure. The possibility of paramagnetic impurities of other elements being responsible for the broad line of the industrial carrier (TiO_2 of technical grade) seems to be ruled out by the spectra obtained on analytical grade anatase, TiO_2, displayed in Fig. 9. The same temperature-sensitive broad line is observed and, additionally, the spectra at high temperatures reveal features of hyperfine structure (insert) possibly caused by the presence of the isotopes ^{47}Ti ($I = 5/2$) and ^{49}Ti ($I = 7/2$) with a natural abundance of 7.3% and 5.5%, respectively, (the dominant isotope ^{48}Ti has nuclear spin $I = 0$) or by paramagnetic oxide species formed by absorption of O_2 in TiO_2 [18]. Preliminary EPR investigations of WO_3 (Merck, pure) reveal a weak and very broad signal similar to TiO_2, without hyperfine structure too, but with an additional narrow signal at $g = 2.002$ close to g_e as expected for an *F*-center [18]. This is probably also caused by non-stoichiometry of WO_3, as for TiO_2, leading to the presence of paramagnetic W species of lower oxidation state than +VI in the bulk of WO_3. It, probably does not contribute to the spectra in Figs. 6 and 7 of the WO_3 promoted V_2O_5/TiO_2 catalyst, since only surface and no bulk species of diamagnetic W(VI) are found in the catalyst (Fig. 10).

3.3. PILC catalysts

The schematic structure of PILC is shown in Fig. 11. Zeolites, e.g. ZSM-5, have a pore structure of 9 Å in cavities and 5.5 Å in channels, whereas pillared clays have much larger pore openings, normally in the range of 8–20 Å [26] making mass-transport restrictions less severe. The height of the pillars are obtained by lowering the basal spacing with thickness of one clay layer, 9.6 Å. The prepared Al-PILC and the LaAl-PILC have been ion exchanged with the transition-metal cations

Cu^{2+}, Cr^{3+}, Ni^{2+} and V^{5+}. The V^{5+} exchange was not successful, but the three remaining successfully metal ion exchanged PILCs were investigated with respect to their catalytic activity for the SCR reaction. The gas mixture employed consisted of 500 ppm NO, 500 ppm NH_3, 2% O_2 and N_2 to balance. The results are displayed in Fig. 12. The four investigated PILCs show substantial activity with respect to NO conversion. The Cu^{2+}exchanged PILCs exhibit somewhat higher activity than the Cr^{3+} and Ni^{2+} exchanged PILCs. The two Cu^{2+} exchanged PILCs exhibit almost the same activity, independent of the PILC being prepared from Al-PILC or the LaAl-PILC (in wet gas, i.e. 7% H_2O). Preliminary EPR measurements on the Cu ion-exchanged PILC show that indeed Cu^{2+} ions are present in the structure. The spectra reveal the characteristic features of Fe^{3+} from the parent clay, i.e. a line at $g \approx 4.22$ and a broad line around $g = 2$, in addition to the characteristic anisotropic spectra ($g_{||} = 2.519$ and $g_{\perp} = 2.101$) of Cu^{2+} bonded — due to the calcination — to oxygen in the silicate layers or the pillars [27]. The temperature of maximum activity is in the range 350–400°C for all catalysts, but the Cu-LaAl-PILC has an appreciable activity (40%) at temperatures as low as 250°C.

Compared to the traditional V_2O_5/TiO_2 based SCR catalyst, however, the PILCs prepared here have much lower activity (<10%). Attempts to improve the ion-exchange procedure to get higher metal content and SCR activity are in progress.

Acknowledgements

The Danish National Research Councils, the EEC program Human Capital and Mobility (contract ERBCHBGCT920129), NATO (sfp971984) and ICAT (Interdisciplinary Center for Catalysis) at the Technical University of Denmark, are thanked for financial support. N.-Y. Topsøe, Haldor Topsøe Research Laboratories, is acknowledged for providing us with the V_2O_5/TiO_2 catalyst. Rikke Mattsson Bruun, Technical University of Denmark, is thanked for experimental assistance.

References

[1] J.H. Frazer, W.J. Kirkpatrick, J. Am. Chem. Soc. 62 (1940) 1659.
[2] H.F.A. Topsøe, A. Nielsen, Trans. Dan. Acad. Tech. Sci. 1 (1947) 18.
[3] J. Villadsen, H. Livbjerg, Catal. Rev.-Sci. Eng. 17 (1978) 203.
[4] N.H. Hansen, R. Fehrmann, N.J. Bjerrum, Inorg. Chem. 21 (1982) 744.
[5] S. Boghosian, R. Fehrmann, N.J. Bjerrum, G.N. Papatheodorou, J. Catal. 119 (1989) 121.
[6] K. Nielsen, K.M. Eriksen, R. Fehrmann, Inorg. Chem. 32 (1993) 4825.
[7] O.B. Lapina, V.M. Mastikhin, A.A. Shubin, K.M. Eriksen, R. Fehrmann, J. Molec. Catal. 99 (1995) 123.
[8] S. Boghosian, F. Borup, A. Chrissanthopoulos, Catal. Lett. 48 (1997) 145.
[9] A. Chrissanthopoulos, F. Borup, R. Fehrmann, S. Boghosian, in preparation.
[10] K.M. Eriksen, D.A. Karydis, S. Boghosian, R. Fehrmann, J. Catal. 155 (1995) 32.
[11] C. Oehlers, R. Fehrmann, S.G. Masters, K.M. Eriksen, D.E. Sheinin, B.S. Bal'zhinimaev, V.I. Elokhin, Appl. Catal. 147 (1996) 127.
[12] S.G. Masters, A. Chrissanthopoulos, K.M. Eriksen, S. Boghosian, R. Fehrmann, J. Catal. 166 (1997) 16.
[13] N.-Y. Topsøe, Science 265 (1994) 1217.
[14] J.B. Miller, S.J. DeCanio, J.B. Michel, C. Dybowski, J. Phys. Chem. 89 (1985) 2592.
[15] J.A. Odriozola, J. Soria, G.A. Somorjai, H. Heinemann, J.F. Garcia de la Banda, M. Lopez Granados, J.C. Conesa, J. Phys. Chem. 95 (1991) 240.
[16] R.B. Bjorklund, L.A.H. Andersson, C.U.I. Odenbrand, L. Sjöqvist, A. Lund, J. Phys. Chem. 96 (1992) 10953.
[17] E.C. Alyea, L.J. Lakshmi, Z. Ju, Langmuir 13 (1997) 5621.
[18] P.F. Cornaz, J.H.C. van Hooff, F.J. Pluijm, G.C.A. Schuit, J. Chem. Soc. Faraday Discuss. 41 (1966) 291.
[19] P. Meriaudeau, M. Che, P.C. Gravelle, S.J. Teichner, Bull. Soc. Chim. Fr. 1 (1971) 13.
[20] R.T. Yang, J.P. Chen, E.S. Kikkidines, L.S. Cheng, Ind. Eng. Chem. Res. 31 (1992) 1440.
[21] J. Sterte, Catal. Today 2 (1988) 219.
[22] H.Y. Zhu, E.F. Vansant, J. Porous Mat. 2 (1995) 107.
[23] D.A. Karydis, K.M. Eriksen, R. Fehrmann, S. Boghosian, J. Chem. Soc. Dalton Trans. 14 (1994) 2151.
[24] O.B. Lapina, B.S. Bal'zhinimaev, S. Boghosian, K.M. Eriksen, R. Fehrmann, Catal. Today 51 (1999) 469.
[25] A. Davidson, M. Che, J. Phys. Chem. 96 (1992) 9909.
[26] M. Shelef, Chem. Rev. 95 (1995) 209.
[27] K. Bahranowski, R. Dula, M. Labanowski, E.M. Serwicka, Appl. Spectrosc. 50 (1996) 1439.